Clinical and Translational Radiation Oncology 45 (2024) 100718

Contents lists available at ScienceDirect

Clinical and Translational Radiation Oncology

journal homepage: www.sciencedirect.com/journal/clinical-and-translational-radiation-oncology

How to contour the different heart subregions for future deep-learning modeling of the heart: A practical pictorial proposal for radiation oncologists

Loig Vaugier [a,*], Elvire Martin-Mervoyer [b], Loic Ah-Thiane [a], Martin Langé [a], Luc Ollivier [a], Tanguy Perennec [a], Stéphane Supiot [a,c], Loig Duvergé [d], François Lucia [e], Pierre Trémolières [f], Roshanack Movassaghi [g], Karine Fresse-Warin [h], Alexandra Moignier [i], Francois Thillays [a]

[a] Department of Radiation Oncology, Institut de Cancérologie de l'Ouest, 44800 Saint Herblain, France
[b] Department of Cardiology, Institut de Cancérologie de l'Ouest, 44800 Saint Herblain, France
[c] Laboratoire US2B, Unité en Sciences Biologiques et Biotechnologies, UMR CNRS 6286, UFR Sciences et Techniques, 2, rue de la Houssinière, 44322 Nantes, France
[d] Department of Radiation Oncology, Centre Eugène Marquis, 35000 Rennes, France
[e] Department of Radiation Oncology, Centre Hospitalo-Universitaire (CHU), 29200 Brest, France
[f] Department of Radiation Oncology, Institut de Cancérologie de l'Ouest, 49000 Angers, France
[g] Department of Radiology, Institut de Cancérologie de l'Ouest, 44800 Saint Herblain, France
[h] Department of Radiology – Non-invasive Cardiovascular Imaging, Centre Hospitalo-Universitaire (CHU), 44000 Nantes, France
[i] Department of Medical Physics, Institut de Cancérologie de l'Ouest, 44800 Saint Herblain, France

ARTICLE INFO

Keywords:
Heart subregions
Delineation
Automatic modeling
Radio-induced cardiotoxicity
Radiotherapy

ABSTRACT

There are currently no accurate rules for manually delineating the subregions of the heart (cavities, vessels, aortic/mitral valves, Planning organ at Risk Volumes for coronary arteries) with the perspective of deep-learning based modeling. Our objective was to present a practical pictorial view for radiation oncologists, based on the RTOG atlas and anatomical complementary considerations for the cases where the RTOG guidelines are missing.

1. Introduction

Better managing the heart and related events following thoracic radiotherapy (RT), is a milestone for next-generation radiation oncologists [1]. Major technical progress in both radiation techniques and in computational approaches have made such ambitions realistic in the near future.

Examining the dose of radiation to the heart in conjunction with the occurrence of cardiovascular events (CVE) is clearly relevant [2,3]. Radio-induced toxicities several years after thoracic RT – mainly coronary artery disease, valvular disease, conduction abnormalities, arrhythmias or interstitial myocardial fibrosis [1] – were mainly shown in breast cancer and Hodgkin lymphoma patients, with the risk depending on the average heart dose [4,5]. More recently, the desire to go beyond the vision of the heart as a single homogenous organ has grown, and tremendous effort has been put into identifying potential relationships between specific CVE and the doses administered to heart subregions [6,7]. Recent clinical data even reveal that subregions beyond well-identified anatomic structures could be implied in the further toxicity. For example, for lung cancer patients, the radiation dose to the base of the heart (including the left main coronary artery, left anterior descending coronary artery, auriculoventricular node etc.) was shown to be associated with major cardiac events or non-cancer death [8–11], while the risk of further atrial fibrillation could be more specifically attributed to doses to a region including the sino-atrial node [12]. Most of these associations are however known from retrospective analyses [1]. Anatomic structures still remain the bricks, and robust definitions are thus required.

A first important step in delineating the heart was reached when the atlases making homogeneization possible e.g. contouring of the whole heart and large cavities, were published [13–15]. Atlases and deep learning-based models have since been elaborated, while manual delineation commonly remains the first step, followed by training of the model on several cases. The results were encouraging for cardiac

* Corresponding author.
E-mail address: loig.vaugier@ico.unicancer.fr (L. Vaugier).

https://doi.org/10.1016/j.ctro.2023.100718
Received 24 January 2023; Received in revised form 14 December 2023; Accepted 16 December 2023
Available online 18 December 2023

chambers and large vessels for example, but delineating the coronary arteries still remains the hardest task [16–18]. The heart's motion, the size and displacement of small structures such as the coronary arteries, and the lack of contrast enhancement between cardiac cavities, are some of the difficulties. In particular, the heart's motion can significantly affect all parts of the heart, and especially the coronary arteries [19,20]. It is furthermore critical that it is considered during RT as the duration of one fraction (typically a few minutes) leads to an average of over a hundred heart pulses. However, neither current atlases nor guidelines propose any practical clues in this regard. Attempts to define high-risk zones for the coronary arteries have already been developed but more specifically in the cases of breast cancer patients with volumes derived from non-contrast enhanced computed tomography [21,22]. Comparisons between atlases and observers reveal the difficulties in getting reproducible contours in the cases of coronary arteries, sino-atrial or auriculoventricular nodes [18]. The absence of "step-by-step" guidelines thus generates inter- and intra-observer variabilities in the manual delineation procedure, causing potential noise that remains one of the main pitfalls for effective automatic segmentation.

Our objective was thus to develop a set of accurate "step-by-step" manual segmentation rules for heart subregions to prepare the further construction of deep learning-based automatic modeling.

2. Materials and methods

Chest contrast-enhanced computed tomography (CE-CT) scans (supine with both arms above the head) from the Institut de Cancérologie de l'Ouest, Saint Herblain, France, were extracted for a first set of 10 patients who also had coronary CT scans with cardiac gating. CE-CT scan slice thickness was 3 mm, and they were registered with the coronary CT scan for all 10 patients. All the CTs were reviewed by both radiation oncologists and cardiologists to establish appropriate rules for segmenting the heart and subregions, based on the RTOG's heart atlas [14] and anatomical considerations for the cases where guidelines were missing [23]. Volumes were contoured using the treatment planning system RayStation (version 10B; RaySearch Laboratories, Stockholm, Sweden). For the coronary arteries, the coronary CTs gave a first view of the arteries' position. Motion was then taken into account by including the coronary artery volume defined on the CE-CT, in all the contrast enhancements seen in the vicinity of the frozen picture obtained from the coronary CT – thus generating a probabilistic Planning organ at Risk Volume (PRV) for the coronary arteries. Once the appropriate segmentation rules were defined, a second set of 10 chest CE-CTs was reviewed to test the feasibility and reproducibility of the segmentation rules. Once the definitions converged after reviewing the 20 patients, they were all approved by a commitee of radiologists and radiation oncologists from various French health care centers.

Our institution has an approved and standardized informed consent process that includes research and access to data. All patients were informed to ensure their non-opposition to the use of their data for research purposes and informed consent was obtained from all participants. The entire study was performed in accordance with the relevant guidelines and regulations.

3. Results

Heart cavities, large vessels, aortic and mitral valves (Table 1), and PRV for the coronary arteries (Table 2), can be delineated separately in a first round, but an adjustment between all the structures is then needed to obtain coherent overall segmentation (Fig. 5). A priority order of segmentation is proposed in Table 3 to make the entire delineation process easier.

3.1. Heart

At the upper level, heart volume starts where the pulmonary trunk and the right pulmonary artery are seen as separate structures, as also suggested in the recent collaborative group of Radiation Therapy Quality Assurance [24]. In practice, one slice of 3 mm below the pulmonary artery trunk crosses the middle line (Fig. 1).

Table 1
Subregion definitions: whole heart, large vessels (in gray), heart cavities and mitral valve, left ventricle wall and interventricular septum (in gray).

Substructure	Window (HU)	Cranial	Caudal	Other limits
Heart	50–500	Pulmonary artery trunk crossing midline (one slice below)	Last slice in the coronal view	
Pulmonary Arteries (PA)	50–150	1st slice with the PA in the axial view	RV	
Superior Vena Cava (SVC)	50–150	Top of the PA	Top of the LV	
Inferior Vena Cava (IVC)	50–150	1st slice of the vena outside the heart	Top of the liver	
Ascending Aorta (AA)	50–150	Top of the PA	Top of the AR	Priority over PA
Aortic Root (AR)	50–150	Top of the coronary arteries in the coronal view	Last slice in the coronal view	Priority over LV, RV and PA
Pulmonary Veins (PV)	50–150	1st slice in the axial view	Top of the LA	
Left Ventricle (LV)	50–500	1st slice in the coronal view	Last slice in the coronal view	Priority over RV and LA
Right Ventricle (RV)	50–500	Top of the LV	Last slice in the coronal view	Lateral border in the alignement with LV border. Priority with the RA
Left Atrium (LA)	50–500	Top of the middle-distal CXCA	Last slice in the coronal view	Priority over RA
Right Atrium (RA)	50–500	1st slice in the coronal view	Last slice in the coronal view	
Mitral valve	50–500			5 mm automatic expansion between the LV and LA junction, excluded from the AR
Interventricular Septum	50–500			Automatic intersection between the LV wall and RV expansion (1 cm patient's left side and 1 cm posteriorly)

3.2. Large vessels

Large vessels include the pulmonary arteries, ascending aorta, superior and inferior vena cava, and the pulmonary veins. The proximal part of the aorta is included in the aortic root comprising the aortic valve. The aortic root includes the emergence of the coronary arteries and starts at the top of the coronary arteries in the coronal view (Fig. 1). The superior vena cava ends with the first slice of the left ventricle. The pulmonary veins end at the inferior level at the top of the left atrium.

Table 2
Planning organ at Risk Volume (PRV) for the coronary arteries. CE = contrast enhancement.

Substructure	Window (HU)	Cranial	Caudal	Other limits
Left Main Coronary Artery (LMCA)	50–500	1st slice in the coronal view; at the top of the AR	Last slice in the coronal view	Space around the CE excluded from the AR, PA, PV, LV. Laterally ends at the bifurcation with the LADCA and CXCA
Left Anterior Descending Coronary Artery (LADCA)	50–500	1st slice in the coronal view; at the top of the AR	Last slice in the axial view	Space around the CE with a 5 mm brush, excluded from the LMCA, PA, PV, LV, RV
Proximal LADCA	50–500	Top of the LADCA	End of the PA/RV and PV/LV channel	
Middle-distal LADCA	50–500	End of the proximal LADCA	Last slice of the LADCA	
Circumflex Coronary Artery (CXCA)	50–500	At the top of the AR	Last slice in the axial view	Space around the CE with a 4 mm brush excluded from the LMCA, LADCA, PV, LA, LV; mitral valve posteriorly
Proximal CXCA	50–500	Top of the CXCA	1st slice in the coronal view with the descending CXCA at the periphery of the heart	
Middle-distal CXCA	50–500	End of CXCA proximal	Last slice of CXCA	
Right Coronary Artery (RCA)	50–500	1st slice in the coronal view	Last slice in the axial view	Space around the CE with a 5 mm brush, sometimes included in the RA or RV, excluded from the AR.
Proximal RCA	50–500	Top of the RCA	Intersection between RA, RV and AR	
Middle-distal RCA	50–500	Top of the proximal RCA	Last slice of the RCA	

3.3. Heart cavities

We have arbitrarily chosen to give delineation priority for the left cavities over the right cavities and for the ventricles over the atrium. This choice was motivated by the description in the literature of a larger incidence of radio-induced adverse effects arising from the left cavities [1]. The aortic root has priority over the left ventricle to prioritize the coronary arteries. The right ventricle and atrium frontier must be aligned with the left ventricle and atrium frontier (Fig. 2) in the slices where it is difficult to distinguish right ventricle from right atrium. The left atrium starts in the continuity of the pulmonary veins. The upper limit coincides with the upper limit of the middle-distal circumflex coronary artery (Fig. 2). The left ventricle wall is defined by an automatic 8 mm inward distance from the left ventricle structure. The interventricular septum is defined by an automatic intersection between the left ventricle wall and the right ventricle expansion (1 cm posteriorly and on the patient's left side).

Table 3
Proposed priority order for contouring the heart subregions.

Substructure	Contouring order index	Impact
Heart	1	All
Left Ventricle (LV)	2	RV, SVC, PA
Left Main Coronary Artery (LMCA)	3	AA, AR
Left Anterior Descending Coronary Artery (LADCA)		
Pulmonary Arteries (PA)	4	
Superior Vena Cava (SVC)		
Inferior Vena Cava (IVC)		
Ascending Aorta (AA)		
Aortic Root (AR)		
Right Ventricle (RV)		
Circumflex Coronary Artery (CXCA) proximal	5	LA, PV
Left Atrium (LA)	6	
Right Atrium (RA)		
Pulmonary Veins (PV)		
Right Coronary Arteries (RCA)	7	
Mitral valve	8	
Interventricular septum		

3.4. Aortic and mitral valves

The aortic valve is included in the aortic root volume as described in the large vessels section. The mitral valve is defined by the intersection of a 5 mm automatic expansion of both the left ventricle and the left atrium, with the exclusion of the aortic root (Fig. 3).

3.5. Coronary arteries

The PRV were defined using a 4 mm brush according to Duane et al. [14] (Table 2). For the patient's left side coronary arteries (Fig. 2 and Appendix Fig. S1): the left main coronary artery (LMCA) starts at the aortic root and stands between the pulmonary arteries, pulmonary veins, and right and left ventricles. Laterally, the LMCA extends as far as the bifurcation with the PRV of the left anterior descending coronary artery (LADCA) and the circumflex coronary artery (CXCA). LADCA and CXCA are split into proximal and middle-distal parts. Middle and distal parts are grouped together for the convenience of delineation, while isolating the proximal part is easier. Regarding the LADCA: the proximal part ends with the last slice where there is a channel between the pulmonary arteries and the pulmonary veins, or between the right and left ventricles (top of Fig. 2 and Appendix Fig. S2). Regarding the CXCA: the middle-distal part begins with the first slice, where the CXCA descends, reaching the periphery of the heart as better seen in the coronal view (bottom of Fig. 2 and Appendix Fig. S2). Posteriorly, the PRV for the CXCA does not exceed the mitral valve.

For the patient's right side coronary arteries (Fig. 4): the PRV for the right coronary arteries (RCA) starts at the aortic root and goes as far as the periphery of the heart, to the crux of the heart. The PRV may include part of the right ventricle and atrium, depending on motion and where the contrast enhancement stands. The caudal limit of the proximal part of the RCA is defined by the end of the intersection between the right atrium, right ventricle, and aortic root.

3.6. Sinoatrial and auriculoventricular nodes

Identifying sinoatrial (SAN) and atrioventricular (AVN) nodes on CT (a fortiori without cardiac gating) is highly challenging. Several approaches have already been proposed in the literature [12,25,26]

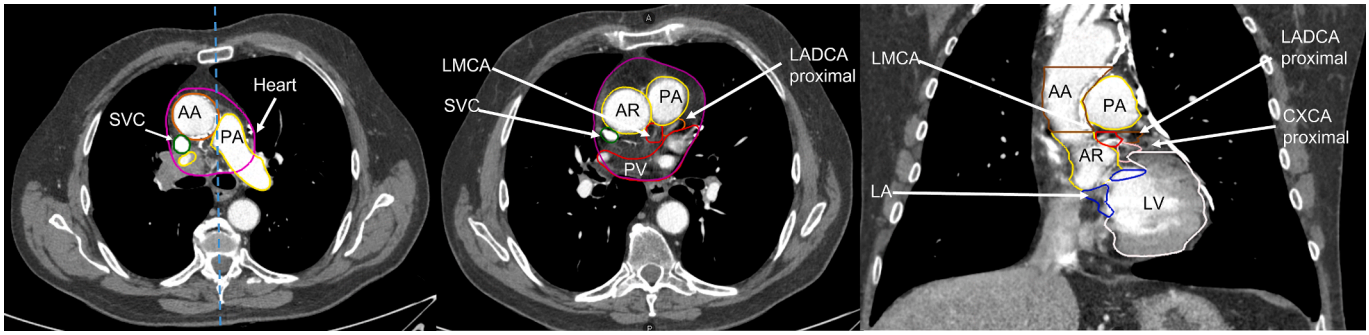

Fig. 1. (color online) Left part: Defining the upper limit of the heart volume (magenta) as the first slice 3 mm below the pulmonary artery trunk crosses the middle line (blue dashed). Middle and right part: Aortic root (proximal part of the aorta and aortic valve). The aortic root starts at the upper level at the top of the coronary arteries' limit in the coronal view. PA = pulmonary arteries (yellow); SVC = superior vena cava (green); AA = ascending aorta (brown); AR = aortic root (yellow); PV = pulmonary veins (red); LV = left ventricle (pink); LA = left atrium (blue); LMCA = left main coronary artery (dark red); planning organ at risk volume (PRV); LADCA = left anterior descending coronary artery (brown); PAV, CXCA = circumflex coronary artery (dark pink) PRV. Levels of 50 HU and a window of 500 HU. (For interpretation of the references to color in this figure legend, the reader is referred to the web version of this article.)

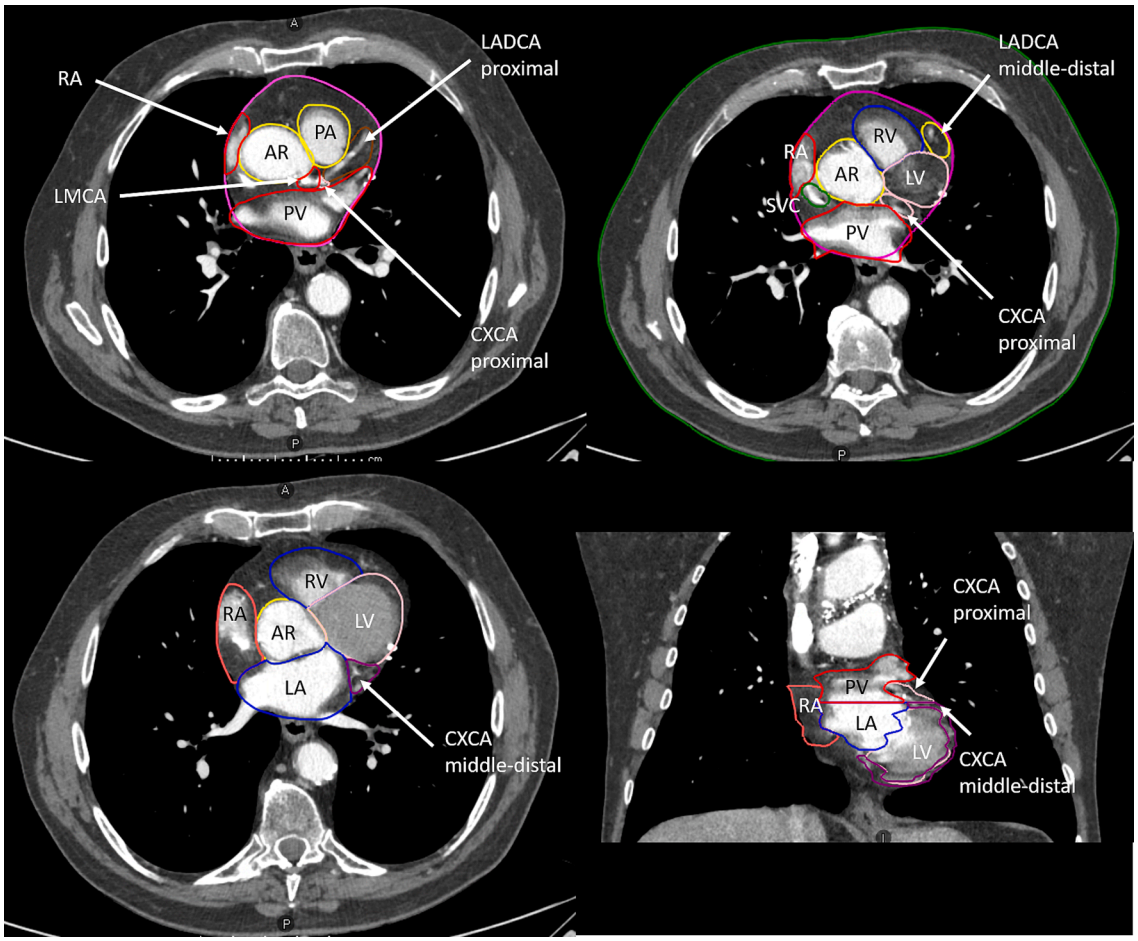

Fig. 2. (color online) Heart cavities and planning organ at risk volumes (PRV) of the left side coronary arteries. Left cavities have priority over right cavities, and ventricle over atrium. The aortic root has priority over the left ventricle. The upper part of the left atrium starts at the top of the middle-distal circumflex coronary artery (with the descending circumflex coronary artery at the periphery of the heart in the coronal view). AR = aortic root (yellow); PA = pulmonary arteries (yellow); PV = pulmonary veins (red); SVC = superior vena cava (green); LV = left ventricle (pink); RV = right ventricle (blue); LA = left atrium (dark blue); RA = right atrium (dark red); LMCA = left main coronary artery (dark red) PRV; LADCA = left-anterior descending coronary artery (proximal: brown, middle-distal: yellow) PRV; CXCA = circumflex coronary artery (proximal: pink, middle-distal: magenta) PRV. (For interpretation of the references to color in this figure legend, the reader is referred to the web version of this article.)

consisting in deriving SAN and AVN from the contours of the large cavities and vessels. These procedures could be thus applied once the large cavities and vessels have been segmented based on the definitions exposed previously.

4. Discussion

Detailed manual segmentation rules for the heart's subregions (heart cavities, large vessels, valves, coronary arteries) with incorporation of

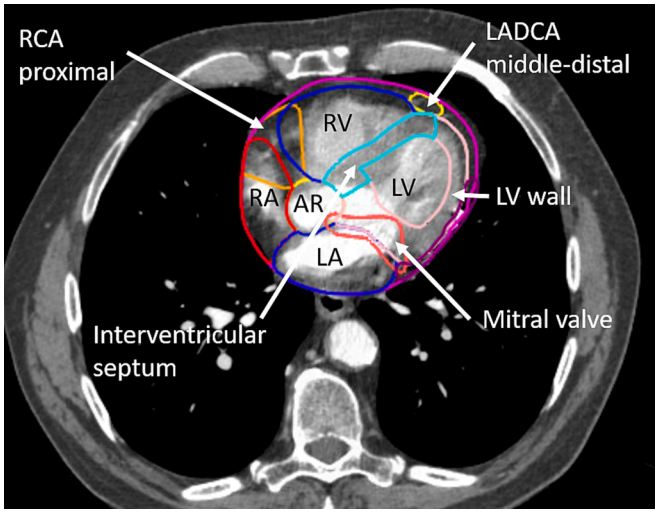

Fig. 3. (color online) Mitral valve, left ventricle wall and interventricular septum. AR = aortic root (yellow); LV = left ventricle (pink); RV = right ventricle (blue); LA = left atrium (dark blue); RA = right atrium (dark red); LADCA = left-anterior descending coronary artery (proximal: brown, middle-distal: yellow); RCA = right coronary artery (orange). (For interpretation of the references to color in this figure legend, the reader is referred to the web version of this article.)

heart motion, are proposed. Such rules will be the bricks for further construction of deep-learning based modeling of the heart. Sinoatrial and atrioventricular nodes could be further defined according to already published approaches, based on appropriate contours for large cavities and vessels. Most of the definitions we have used are coherent with the definitions provided by the RTOG and the Danish Multidisciplinary Cancer Groups. We have added complementary definitions to set i) priority rules for the borders between the cavities or between the cavities and the vessels; ii) a practical order of delineation between the various subregions to make the process easier; iii) a practical approach we referred to as PRV for the segmentation of the coronary arteries, considering their mobility with the motion of the heart and their size.

Using CE-CT appeared to be the first requirement in our approach to i) better identify the borders of the heart and its cavities; ii) better register with the coronary CT; iii) better delineate the volume occupied by the coronary arteries and their motion, leading to the PRV; iv) help in the learning curve process. However, most of the CT used for radiotherapy planning are non-contrast enhanced. Once the automatic segmentation model based on CE-CT becomes effective, the next step will consist in propagating the model of the heart's subregions on both CE- and non CE-CT but for the same patient anatomy.

The resulting motion of the beating heart and breathing lungs is a complex issue in the delineation process of heart subregions. This motion may affect all the subregions, e.g. with displacements observed in the heart cavities from 0.7 to 1 cm and the most significant effects in the case of coronary arteries and valves (from 1.2 to 1.5 cm) according to 4-dimensional CT (4D-CT) analyses [19,20,27]. Approaches based on identifying high-risk zones that play the role of surrogate for e.g. LADCA have been developed in order to get around such issues, but mostly in the perspective of an avoidance zone for dosimetric optimization for breast cancer patients [21]. In our work, we started from coronary CT registered with CE-CT with deep inspiratory apnea first, in order to build PRV similarly to previous studies [22,28] while the heart beats. Such approximation for the coronary arteries could improve the results of further deep learning-based modeling, as it may overcome the sensitivity with the manual contours used for the training. 4D-CT will be considered in the next step in order to deal with the heart motion arising from the breathing lungs.

Our work has obvious limitations. Some of our definitions may appear arbitrary but were all approved by a consensus of expert radiation therapists, radiologists, and cardiologists, and are necessary if the aim is to lay the foundations for future automatic modeling. Using other imaging modalities, such as CT with systematic cardiac gating, would provide better spatial and temporal resolution. Cardiac magnetic resonance imaging (MRI) could also be interesting [29] but this leads to other difficulties, such as CT/MRI registration or access to imaging technology, while the MRI spatial resolution is still lower compared to CT with cardiac gating. Other alternative strategies have investigated heart toxicity without systematic contouring of the heart subregions but by using representative anatomies instead and voxel-wise analysis [7,8]. The authors were able to identify specific subregions beyond an anatomic substrate and encompassing e.g. the base of the heart. A further corresponding anatomic rationale is still necessary to address appropriate follow-up or therapeutic strategy.

5. Conclusion

Reproducible and detailed segmentation rules for the heart's subregions (heart cavities, large vessels, valves, coronary arteries) with incorporation of heart motion, are proposed to build future automatic modeling of the heart.

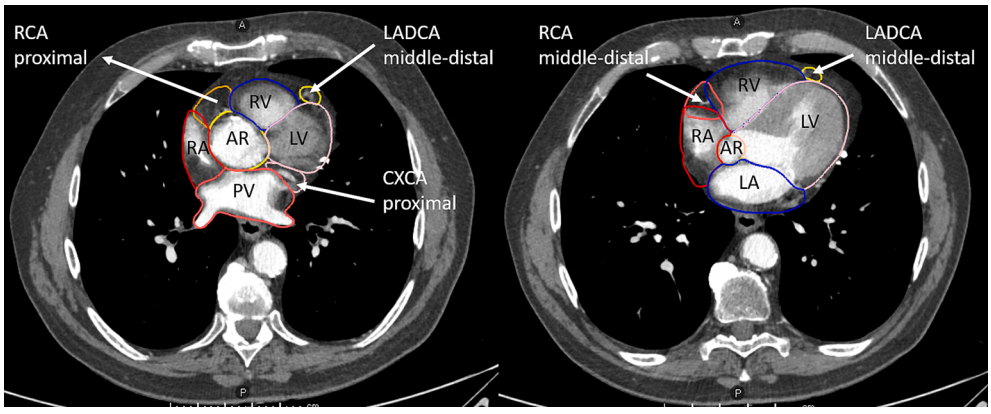

Fig. 4. (color online) Planning organ at risk volume (PRV) of the right-side coronary arteries (RCA). The proximal RCA (orange) ends at the end of the channel between the right ventricle and atrium. The middle-distal RCA (red) follows at the border of the heart and can be inside the right atrium and ventricle, depending on motion. AR = aortic root (yellow); PV = pulmonary veins (red); LV = left ventricle (pink); RV = right ventricle (blue); LA = left atrium (dark blue); RA = right atrium (dark red); LADCA = left-anterior descending coronary artery (yellow) PRV; CXCA = circumflex coronary artery (pink) PRV. (For interpretation of the references to color in this figure legend, the reader is referred to the web version of this article.)

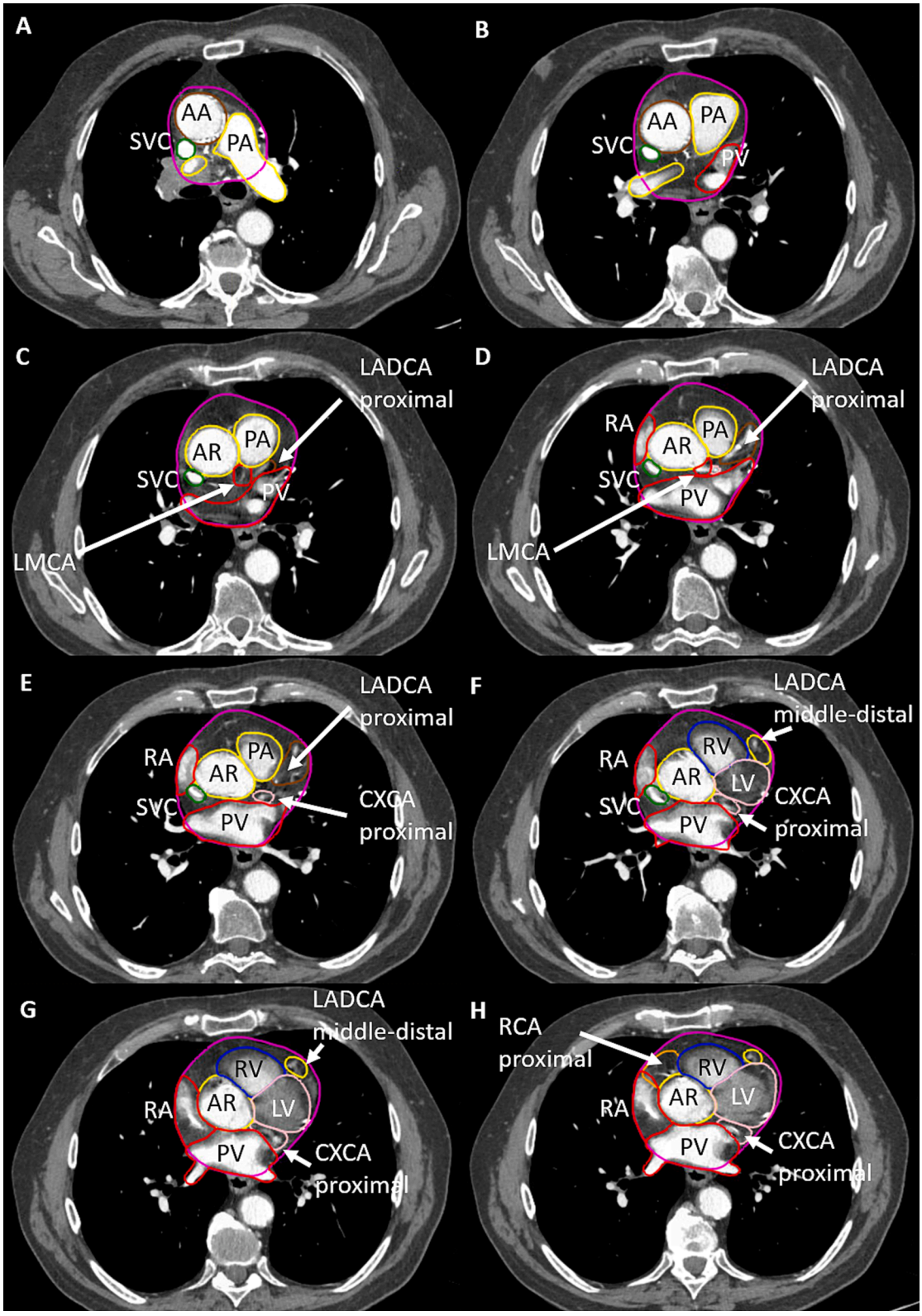

Fig. 5. (From A to P, color online) Heart cavities, large vessels, and planning organ at risk volumes (PRV) of the coronary arteries. AA = ascending aorta (brown); AR = aortic root (yellow); PA = pulmonary arteries (yellow); PV = pulmonary veins (red); SVC = superior vena cava (green); LV = left ventricle (pink); RV = right ventricle (blue); LA = left atrium (dark blue); RA = right atrium (dark red); IVC = inferior vena cava (cyan); LMCA = left main coronary artery (dark red); LADCA = left-anterior descending coronary artery (proximal: brown, middle-distal: yellow); CXCA = circumflex coronary artery (proximal: pink, middle-distal: magenta); RCA = right coronary artery (proximal: orange, middle-distal: red). (For interpretation of the references to color in this figure legend, the reader is referred to the web version of this article.)

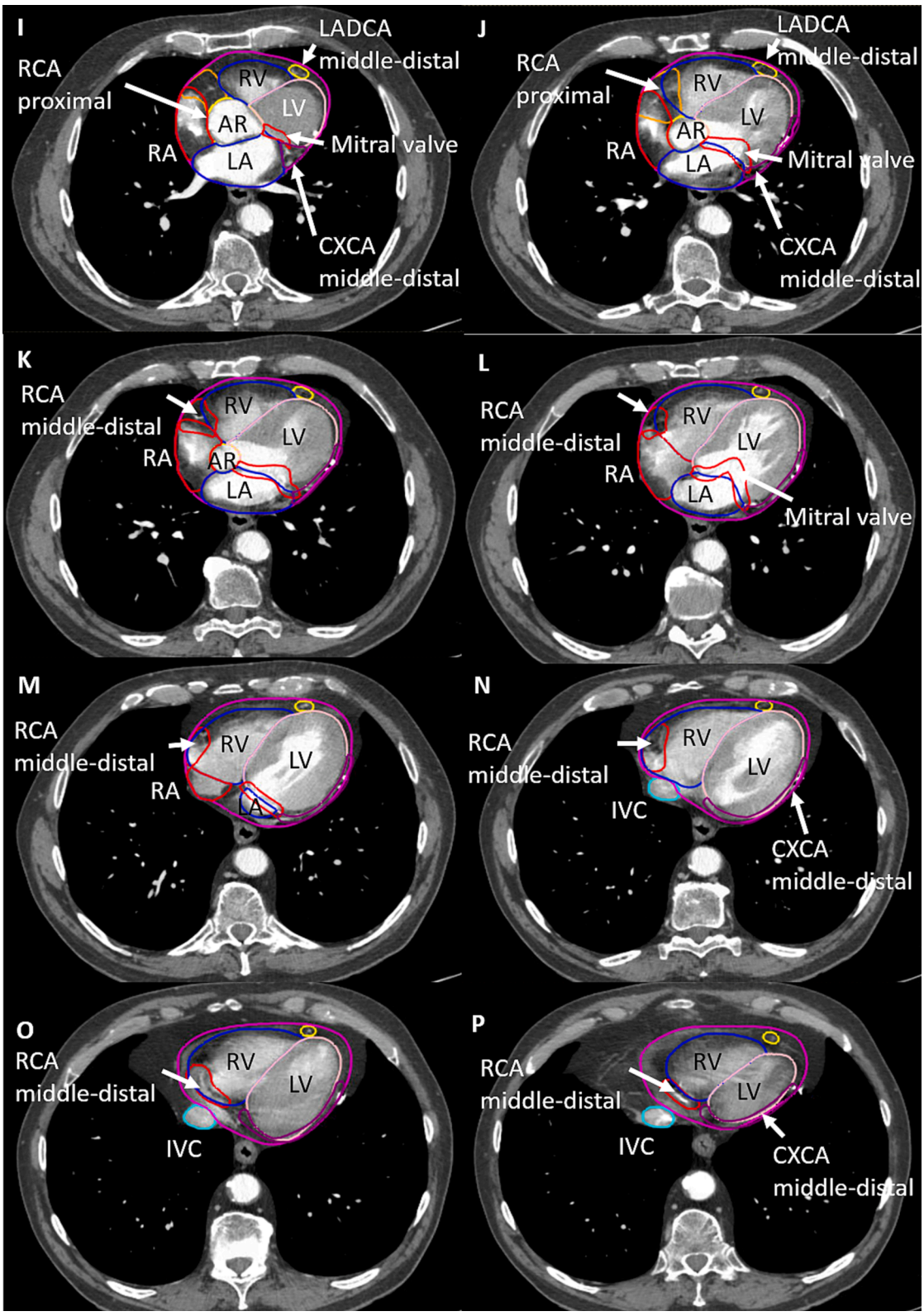

Fig. 5. (*continued*).

Conflict of interests

None.

CRediT authorship contribution statement

Loig Vaugier: Conceptualization, Data curation, Formal analysis, Investigation, Methodology, Supervision, Writing – original draft, Writing – review & editing. **Elvire Martin-Mervoyer:** Conceptualization, Formal analysis, Investigation, Methodology, Supervision, Writing

– review & editing. **Loic Ah-Thiane:** Writing – review & editing. **Martin Langé:** Writing – review & editing. **Luc Ollivier:** Writing – review & editing. **Tanguy Perennec:** Writing – review & editing. **Stéphane Supiot:** Writing – review & editing. **Loig Duvergé:** Writing – review & editing. **François Lucia:** Writing – review & editing. **Pierre Trémolières:** Writing – review & editing. **Roshanack Movassaghi:** Writing – review & editing. **Karine Fresse-Warin:** Investigation, Methodology, Writing – review & editing. **Alexandra Moignier:** Conceptualization, Data curation, Formal analysis, Investigation, Methodology, Supervision, Writing – review & editing. **Francois Thillays:** Conceptualization, Formal analysis, Investigation, Methodology, Supervision, Writing – review & editing.

Declaration of competing interest

The authors declare that they have no known competing financial interests or personal relationships that could have appeared to influence the work reported in this paper.

Acknowledgments

We would like to thank RaySearch Laboratories AB (Stockholm, Sweden) for their contribution to the development of the deep learning model dedicated to heart substructures. This work is preliminary to our partnership.

Appendix A. Supplementary data

Supplementary data to this article can be found online at https://doi.org/10.1016/j.ctro.2023.100718.

References

[1] Banfill K, Giuliani M, Aznar M, Franks K, McWilliam A, Schmitt M, et al. Cardiac toxicity of thoracic radiotherapy: existing evidence and future directions. J Thorac Oncol 2021;16:216–27.
[2] Nordsmark M, Offersen BV. The risk of radiation-associated heart disease comes from many factors; the chain is as strong as the weakest link. Radiother Oncol 2020;152:101–2.
[3] Raghunathan D, Khilji MI, Hassan SA, Yusuf SW. Radiation-induced cardiovascular disease. Curr Atheroscler Rep 2017;19:22.
[4] Darby SC, Ewertz M, McGale P, Bennet AM, Blom-Goldman U, Brønnum D, et al. Risk of ischemic heart disease in women after radiotherapy for breast cancer. N Engl J Med 2013;368:987–98.
[5] van Nimwegen FA, Ntentas G, Darby SC, Schaapveld M, Hauptmann M, Lugtenburg PJ, et al. Risk of heart failure in survivors of Hodgkin lymphoma: effects of cardiac exposure to radiation and anthracyclines. Blood 2017;129:2257–65.
[6] Trivedi SJ, Tang S, Byth K, Stefani L, Lo Q, Otton J, et al. Segmental cardiac radiation dose determines magnitude of regional cardiac dysfunction. J Am Heart Assoc 2021;10:e019476.
[7] McWilliam A, Khalifa J, Vasquez Osorio E, Banfill K, Abravan A, Faivre-Finn C, et al. Novel methodology to investigate the effect of radiation dose to heart substructures on overall survival. Int J Radiat Oncol 2020;108:1073–81.
[8] McWilliam A, Abravan A, Banfill K, Faivre-Finn C, van Herk M. Demystifying the Results of RTOG 0617: Identification of Dose Sensitive Cardiac Subregions Associated With Overall Survival. J Thorac Oncol. 2023;S1556086423000941.
[9] McKenzie E, Zhang S, Zakariaee R, Guthier CV, Hakimian B, Mirhadi A, et al. Left Anterior Descending Coronary Artery Radiation Dose Association with All-Cause Mortality in NRG Oncology Trial RTOG 0617. Int J Radiat Oncol. 2022;S0360301622035659.
[10] Atkins KM, Chaunzwa TL, Lamba N, Bitterman DS, Rawal B, Bredfeldt J, et al. Association of left anterior descending coronary artery radiation dose with major adverse cardiac events and mortality in patients with non-small cell lung cancer. JAMA Oncol 2021;7:206.
[11] Stam B, Peulen H, Guckenberger M, Mantel F, Hope A, Werner-Wasik M, et al. Dose to heart substructures is associated with non-cancer death after SBRT in stage I-II NSCLC patients. Radiother Oncol 2017;123:370–5.
[12] Kim KH, Oh J, Yang G, Lee J, Kim J, Gwak S, et al. Association of sinoatrial node radiation dose with atrial fibrillation and mortality in patients with lung cancer. JAMA Oncol 2022;8:1624.
[13] Feng M, Moran JM, Koelling T, Chughtai A, Chan JL, Freedman L, et al. Development and validation of a heart atlas to study cardiac exposure to radiation following treatment for breast cancer. Int J Radiat Oncol Biol Phys 2011;79:10–8.
[14] Duane F, Aznar MC, Bartlett F, Cutter DJ, Darby SC, Jagsi R, et al. A cardiac contouring atlas for radiotherapy. Radiother Oncol 2017;122:416–22.
[15] Milo MLH, Offersen BV, Bechmann T, Diederichsen ACP, Hansen CR, Holtved E, et al. Delineation of whole heart and substructures in thoracic radiation therapy: National guidelines and contouring atlas by the Danish Multidisciplinary Cancer Groups. Radiother Oncol 2020;150:121–7.
[16] Garrett Fernandes M, Bussink J, Stam B, Wijsman R, Schinagl DAX, Monshouwer R, et al. Deep learning model for automatic contouring of cardiovascular substructures on radiotherapy planning CT images: Dosimetric validation and reader study based clinical acceptability testing. Radiother Oncol 2021;165:52–9.
[17] van den Oever LB, Spoor DS, Crijns APG, Vliegenthart R, Oudkerk M, Veldhuis RNJ, et al. Automatic cardiac structure contouring for small datasets with cascaded deep learning models. J Med Syst 2022;46:22.
[18] Loap P, De Marzi L, Kirov K, Servois V, Fourquet A, Khoubeyb A, et al. Development of simplified auto-segmentable functional cardiac atlas. Pract Radiat Oncol 2022;12:533–8.
[19] Socha J, Rygielska A, Uziębło-Życzkowska B, Chałubińska-Fendler J, Jurek A, Maciorowska M, et al. Contouring cardiac substructures on average intensity projection 4D-CT for lung cancer radiotherapy: A proposal of a heart valve contouring atlas. Radiother Oncol 2022;167:261–8.
[20] Guzhva L, Flampouri S, Mendenhall NP, Morris CG, Hoppe BS. Intrafractional displacement of cardiac substructures among patients with mediastinal lymphoma or lung cancer. Adv Radiat Oncol 2019;4:500–6.
[21] Loap P, Tkatchenko N, Nicolas E, Fourquet A, Kirova Y. Optimization and auto-segmentation of a high risk cardiac zone for heart sparing in breast cancer radiotherapy. Radiother Oncol 2020;153:146–54.
[22] Lee J, Hua K-L, Hsu S-M, Lin J-B, Lee C-H, Lu K-W, et al. Development of delineation for the left anterior descending coronary artery region in left breast cancer radiotherapy: An optimized organ at risk. Radiother Oncol 2017;122:423–30.
[23] Gopal A. Cardiac anatomy by computed tomographic imaging. London; 2008.
[24] Mir R, Kelly SM, Xiao Y, Moore A, Clark CH, Clementel E, et al. Organ at risk delineation for radiation therapy clinical trials: Global Harmonization Group consensus guidelines. Radiother Oncol 2020;150:30–9.
[25] Loap P, Servois V, Dhonneur G, Kirov K, Fourquet A, Kirova Y. A radiation therapy contouring atlas for cardiac conduction node delineation. Pract Radiat Oncol 2021;11:e434–7.
[26] Qian Y, Zhu H, Pollom EL, Durkee BY, Chaudhuri AA, Gensheimer MF, et al. Sinoatrial node toxicity after stereotactic ablative radiation therapy to lung tumors. Pract Radiat Oncol 2017;7:e525–9.
[27] Walls GM, Giacometti V, Apte A, Thor M, McCann C, Hanna GG, et al. Validation of an established deep learning auto-segmentation tool for cardiac substructures in 4D radiotherapy planning scans. Phys Imaging Radiat Oncol 2022;23:118–26.
[28] Munshi A, Khataniar N, Sarkar B, Bera ML, Mohanti BK. Spatial orientation of coronary arteries and its implication for breast and thoracic radiotherapy—proposing "coronary strip" as a new organ at risk. Strahlenther Onkol 2018;194:711–8.
[29] Morris ED, Ghanem AI, Pantelic MV, Walker EM, Han X, Glide-Hurst CK. Cardiac substructure segmentation and dosimetry using a novel hybrid magnetic resonance and computed tomography cardiac atlas. Int J Radiat Oncol Biol Phys 2019;103:985–93.